

Article

A Nonbinary LDPC-Coded Probabilistic Shaping Scheme for a Rayleigh Fading Channel

Weimin Kang 

School of Information and Communication Engineering, North University of China, Taiyuan 030051, China; kwm2013@126.com

Abstract: In this paper, a novel, nonbinary (NB) LDPC-coded probabilistic shaping (PS) scheme for a Rayleigh fading channel is proposed. For the NB LDPC-coded PS scheme in Rayleigh fading channel, the rotation angle of 16 quadrature amplitude modulation (QAM) constellations, 64QAM constellations and 256QAM constellations are optimized by the exhaustive search. The simulation results verify the information–theoretical analysis. Compared with the binary LDPC-coded PS scheme for Rayleigh fading channel, the proposed NB LDPC-coded PS scheme can improve error performance. In summary, the proposed NB LDPC-coded PS scheme for Rayleigh fading channel is reliable and thus suitable for future communication systems.

Keywords: probabilistic shaping; nonbinary LDPC; Rayleigh fading

1. Introduction

High spectral efficiency (SE) is required in future communication systems, where advanced channel coding schemes and high-order modulation formats play an important role [1–3]. In most conventional practical communication systems, when using the uniformly distributed quadrature amplitude modulation (QAM) constellations, it will cause a loss of up to $\pi e/6$ (≈ 1.53 dB) toward the Shannon limit [4]. In order to obtain a shaping gain, a probabilistic shaping (PS) scheme was proposed in [5], which utilizes a constant composition distribution matcher (CCDM) [6] to generate different amplitude probability distributions. In [7,8], a binary LDPC-coded rotated QAM-based PS scheme for Rayleigh fading channel was proposed, where a rate 5/6 binary LDPC code was used for both the PS-rotated QAM scheme and the uniform-rotated QAM scheme. The PS scheme would bring rate loss. Therefore, the bit-error-rate (BER) performance, which is examined in [7,8], is not calculated on the basis of SE since the SE changes for different modulation schemes in [7,8]. Therefore, we should evaluate the PS scheme with the same SE and verify the PS gain for the Rayleigh fading channel. For the fading channel, diversity is an efficient method against fading [9]. Constellation rotation can obtain diversity gain for the fading channel, which is widely used for wireless communication standards.

In general, the LDPC codes exhibit better behavior for high code rates when they are compared to turbo codes. In a 5G long code block coding scheme, the LDPC code is used for enhanced mobile broadband service data information. Compared to the binary LDPC codes, the nonbinary (NB) LDPC codes [10] over Galois field $GF(q)$ show better error performance for short blocks. $q = 2^p$, where p represents the number of symbolic quantization bits. The NB LDPC-coded PS scheme for an additive white Gaussian noise (AWGN) channel shows excellent error performance in [11,12]. In order to use a flexible LDPC code rate, a NB LDPC-coded hybrid probabilistic shaping scheme was proposed in [13]. However, this work is assumed on an additive white Gaussian noise (AWGN) channel. Considering the wireless fading channel, it is an important issue to evaluate the NB LDPC-coded PS scheme for Rayleigh fading channel and optimize the rotation angle of QAM signals to obtain diversity gain.



Citation: Kang, W. A Nonbinary LDPC-Coded Probabilistic Shaping Scheme for a Rayleigh Fading Channel. *Entropy* **2022**, *24*, 1649. <https://doi.org/10.3390/e24111649>

Academic Editors: Jun Chen and Sadaf Salehkalaibar

Received: 28 September 2022

Accepted: 12 November 2022

Published: 14 November 2022

Publisher's Note: MDPI stays neutral with regard to jurisdictional claims in published maps and institutional affiliations.



Copyright: © 2022 by the authors. Licensee MDPI, Basel, Switzerland. This article is an open access article distributed under the terms and conditions of the Creative Commons Attribution (CC BY) license (<https://creativecommons.org/licenses/by/4.0/>).

In this paper, we propose a NB LDPC-coded PS scheme for Rayleigh fading channel and optimize the rotation angle of QAM signals by the exhaustive search. The theoretical average mutual information (AMI) analysis and simulation error performance show the reliability of the proposed scheme.

The innovation of this paper is shown as follows.

- A NB LDPC-coded two-dimensional PS scheme for Rayleigh fading channel is proposed. Compared with the binary LDPC-coded two-dimensional PS scheme in [7], the proposed NB LDPC-coded two-dimensional PS scheme can obtain coding gain.
- A NB LDPC-coded two-dimensional QAM PS scheme for Rayleigh fading channel based on signal space diversity is proposed. Compared to the NB LDPC-coded two-dimensional QAM PS scheme for Rayleigh fading channel without rotation, the proposed NB LDPC-coded two-dimensional QAM PS scheme for Rayleigh fading channel based on signal space diversity can obtain diversity gain.

The rest of the paper is organized as follows. In Section II, the system model of the NB LDPC-coded PS scheme for Rayleigh fading channel is proposed. AMI analysis of the proposed PS scheme for Rayleigh fading channel is discussed in Section III. In Section IV, simulation results are shown. Conclusions are given in Section V.

2. Methods

The proposed NB LDPC-coded PS scheme for Rayleigh fading channel is shown in Figure 1. In the transmitter, a length of k uniform data bits u_{bin}^A is used for generating the nonuniform n amplitude symbols according to the unequal probability distribution $P_{\bar{A}}$, which is generated by distribution matcher (DM). For Gray-labeled QAM constellations, such as 16QAM, 64QAM and 256QAM constellations, we consider using two-dimensional PS. Hereby, we use two \sqrt{M} -ASK constellations for one M-QAM constellation. Let $\chi_{\bar{A}}(\cdot)$ denote the amplitude labeling function, where $\chi_{\bar{A}} : \bar{A} \rightarrow \{0, 1\}^{m-1}$, $m = \frac{\sqrt{M}}{2}$. Assume the binary bits sequence of one 4-ASK symbol is b_1b_2 , where b_1 denotes the sign bit, and b_2 represents the amplitude bits. The symbols $-$ and $+$ correspond to $b_1 = 0$ and $b_1 = 1$, respectively. The amplitudes 3 and 1 correspond to $b_2 = 0$ and $b_2 = 1$, respectively. Assume the binary bits sequence of one 8-ASK symbol is $b_1b_2b_3$, where b_1 denotes the sign bit, and b_2b_3 represents the amplitude bits. The symbols $-$ and $+$ correspond to $b_1 = 0$ and $b_1 = 1$, respectively. The amplitudes 7, 5, 3 and 1 correspond to $b_2b_3 = 00$, $b_2b_3 = 01$, $b_2b_3 = 11$ and $b_2b_3 = 10$, respectively. Assume the binary bits sequence of one 16-ASK symbol is $b_1b_2b_3b_4$, where b_1 denotes the sign bit, and $b_2b_3b_4$ represents the amplitude bits. The symbols $-$ and $+$ correspond to $b_1 = 0$ and $b_1 = 1$, respectively. The amplitudes 15, 13, 11, 9, 7, 5, 3 and 1 correspond to $b_2b_3b_4 = 000$, $b_2b_3b_4 = 001$, $b_2b_3b_4 = 011$, $b_2b_3b_4 = 010$, $b_2b_3b_4 = 100$, $b_2b_3b_4 = 101$, $b_2b_3b_4 = 111$ and $b_2b_3b_4 = 110$, respectively. For 4-ASK constellations,

$$\chi_{\bar{A}}(3) = 0, \chi_{\bar{A}}(1) = 1. \quad (1)$$

For 8-ASK constellations,

$$\chi_{\bar{A}}(7) = 00, \chi_{\bar{A}}(5) = 01, \chi_{\bar{A}}(3) = 11, \chi_{\bar{A}}(1) = 10. \quad (2)$$

For 16-ASK constellations,

$$\begin{aligned} \chi_{\bar{A}}(15) = 000, \chi_{\bar{A}}(13) = 001, \chi_{\bar{A}}(11) = 011, \chi_{\bar{A}}(9) = 010, \\ \chi_{\bar{A}}(7) = 100, \chi_{\bar{A}}(5) = 101, \chi_{\bar{A}}(3) = 111, \chi_{\bar{A}}(1) = 110. \end{aligned} \quad (3)$$

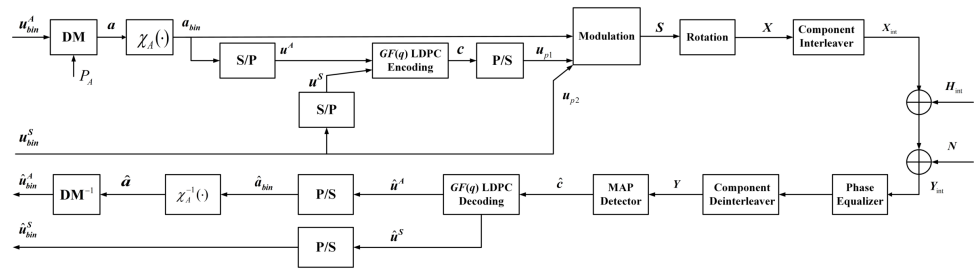


Figure 1. The system model of the proposed NB LDPC-coded probabilistic shaping scheme for Rayleigh fading channel.

The binary data bits a_{bin} are converted into u^A by series-to-parallel (S/P) conversion, which is one part of the $GF(2^p)$ LDPC information symbols. We assume that the $GF(2^p)$ LDPC code rate is r , and the length of information symbols and parity symbols are k_c and $n_c - k_c$, respectively. The length of the additional data source bits u_{bin}^S is $mnr - (m - 1)n$. The total code rate is $R = \frac{k + mnr - (m - 1)n}{mn}$. u_{bin}^S are converted into u^S by S/P conversion, which is the other part of the $GF(2^p)$ LDPC information symbols. The $GF(2^p)$ LDPC codes use systematic encoding with the generator matrix G , which can be obtained by the parity-check matrix H , and the parity-check matrix H is constructed by the progressive edge-growth algorithm [14]. After passing through NB LDPC encoding, the uniformly distributed parity symbols c can be transferred into data bits u_{p1} by parallel-to-series (P/S) conversion. The additional data source bits u_{bin}^S are assumed as u_{p2} , and the connected data sequences $\{u_{p1}, u_{p2}\}$ are used for generating modulated sign parts, while a_{bin} are used for generating modulated amplitude parts. For one \sqrt{M} -ASK constellation symbol, the length of the modulated sign part is one bit, while the length of the modulated sign part is $\frac{\sqrt{M}}{2} - 1$ bits. The signal $X = [X_I, X_Q]^T$ is obtained by the rotation of the traditional signal $S = [S_I, S_Q]^T$, which can be expressed as

$$\begin{bmatrix} X_I \\ X_Q \end{bmatrix} = \begin{bmatrix} \cos \theta & \sin \theta \\ -\sin \theta & \cos \theta \end{bmatrix} \begin{bmatrix} S_I \\ S_Q \end{bmatrix}, \tag{4}$$

where θ is the rotated angle. X_I and X_Q denote the in-phase signal of X and the quadrature signal of X , respectively. In order to improve the reliability performance in fading channels, a component interleaver is used, which can make in-phase and quadrature signals go through different fading. Then, the X_{int} signals can be obtained after the component interleaver. Assume that the receiver can get the perfect channel state information; the received signals can be expressed as

$$Y_{int} = H_{int}X_{int} + N, \tag{5}$$

where N is the complex Gaussian noise with zero mean and variance σ^2 . H_{int} denotes the channel coefficient with zero mean and unit variance.

In the receiver, after passing through the phase equalizer, the received signal is converted into

$$\frac{H_{int}^\dagger}{\|H_{int}\|} Y_{int} = \|H_{int}\| X_{int} + \frac{H_{int}^\dagger}{\|H_{int}\|} N. \tag{6}$$

After the component deinterleaver, the signal $Y = [Y_I, Y_Q]^T$ can be obtained. After maximum a posteriori (MAP) detection, we can get NB LDPC symbol-level log-likelihood ratios. Assume that the label $B = B_1 B_2 \cdots B_p = \text{label}(x_i)$, which means that one $GF(2^p)$ LDPC code corresponds to one QAM symbol. The received noisy symbol y_i is demodulated by calculating $l_{i,j}$,

$$l_{i,j} = \log \frac{P_{B_j}(0)}{P_{B_j}(1)} + \log \frac{q_{i,j}(y_i|0)}{q_{i,j}(y_i|1)}, \tag{7}$$

$$P_{B_j}(b) = \sum_{a \in \{0,1\}^p: a_j=b} P_B(a), \tag{8}$$

$$q_{i,j}(y|b) = \sum_{a \in \{0,1\}^p: a_j=b} q_c(y_i|x_a) \frac{P_B(a)}{P_{B_j}(b)}, \tag{9}$$

where $i = 1, 2, \dots, n_c, j = 1, 2, \dots, p$. $q_c(\cdot|\cdot)$ is a conditional probability density function. $x_a = \{x_{a_I}, x_{a_Q}\}$, x_{a_I} and x_{a_Q} denote the real part of x_a and the image part of x_a , respectively.

$$q_c(y|x_a) = \frac{1}{\sqrt{2\pi\sigma^2}} \exp \frac{-(y_I - |h_I| \cdot x_{a_I})^2 - (y_Q - |h_Q| \cdot x_{a_Q})^2}{2\sigma^2}. \tag{10}$$

The demodulated bit probability is

$$P(y_{i,j} = 0) = \frac{1}{1+\exp(-l_{i,j})}, P(y_{i,j} = 1) = \frac{\exp(-l_{i,j})}{1+\exp(-l_{i,j})}, \tag{11}$$

for $i = 1, 2, \dots, n_c, j = 1, 2, \dots, p$. The GF(2^p) LDPC decoder input is calculated as

$$P_i(c) = \frac{\tilde{P}_i(c)}{\sum_{c' \in GF(2^p)} \tilde{P}_i(c')}, \tilde{P}_i(c) = \prod_{j=1}^p \tilde{P}_{i,j}, \tag{12}$$

for $i = 1, 2, \dots, n_c, j = 1, 2, \dots, p$, where

$$\tilde{P}_{i,j} = \begin{cases} P(y_{i,j} = 0), & \text{if } [\phi_{GF(2^p)}^{-1}(c)]_j = 0 \\ P(y_{i,j} = 1), & \text{if } [\phi_{GF(2^p)}^{-1}(c)]_j = 1 \end{cases} \tag{13}$$

$[\phi_{GF(2^p)}^{-1}(c)]_j$ is the j -th binary mapping bit of c for $c \in GF(2^p)$.

According to [15], the decoding complexity comparison of per bit per iteration for the Log-FFT-BP decoding algorithm of NB LDPC codes and the Log-BP algorithm of binary LDPC codes are shown in Table 1, where d_v denotes the average column weight. The regular GF(256) LDPC codes with $d_v = 2$ and regular GF(2) LDPC codes with $d_v = 3$ are compared, which shows that the decoding complexity comparison of per bit per iteration for the GF(256) LDPC codes is about 144.7 times as much as that of GF(2) LDPC codes.

Table 1. The decoding complexity of Log-FFT-BP and Log-BP per bit per iteration

Operation	Log-FFT-BP for NB LDPC	Log-BP for Binary LDPC	GF(256) Regular LDPC, $d_v = 2, p = 8$	GF(2) Regular LDPC $d_v = 3$
addition/subtraction	$(2q + \frac{4q}{p})d_v$	$4d_v - 1$	1280	11
comparison	$2qd_v$	–	1024	–
table look-up	$2qd_v$	$4d_v$	1024	12
total	$(6q + \frac{4q}{p})d_v$	$8d_v - 1$	3328	23

The NB LDPC decoding symbols sequence \hat{u}^A, \hat{u}^S are then mapped via P/S converter. After $\chi_{\hat{A}}^{-1}(\cdot)$ amplitude inverse labeling function and inverse DM operation, we can finally get the estimated data bits $\{\hat{u}_{bin}^A, \hat{u}_{bin}^S\}$.

3. Average Mutual Information Analysis

The average mutual information (AMI) is the theoretical upper bound, which could be reliably transmitted for given constellation modulation formats. In this section, The regular Nyquist bit-interleaved coded modulation (BICM)-AMI and the PS BICM-AMI for Rayleigh fading channel are investigated. A Gray-labeled M -ary QAM constellation consists of two orthogonal \sqrt{M} -ASK constellations. Considering the \sqrt{M} -ASK constellations, the amplitude probability distribution $P_X(x)$ is selected from Maxwell-Boltzmann (M-B) distribution [7], and $P_X(x) \propto \exp(-vx^2)$, where x denotes amplitude. v represents the non-negative factor, which can determine the system entropy. When $v = 0.0$, it means that the constellation points are subject to a uniform distribution. When $v > 0.0$, it means that the constellation points are subject to nonuniform distribution. In Figure 2, the amplitude probability distribution for 4-ASK is [3:1]=[0.3505: 0.6495], while the amplitude probability distribution for 8-ASK in Figure 3. is subject to [7:5:3:1]=[0.126429:0.213095:0.301666: 0.358810]. In Figure 4, the amplitude probability distribution for 16-ASK is satisfied to [15:13:11:9:7:5:3:1]=[0.0493333: 0.069: 0.0916667:0.116667:0.141333:0.163333:0.18: 0.188667].

The BICM-AMI of the proposed PS system for Rayleigh fading channel can be calculated as

$$\begin{aligned}
 I_{BICM} &= \sum_{i=1}^m I(c_i; y|h) \\
 &= H(x) - \sum_{i=1}^m E_{c_i, y, h} \left[\log_2 \frac{\sum_{\bar{x} \in \mathcal{O}} P(y|\bar{x}, h)P(\bar{x})}{\sum_{x \in \mathcal{O}_{c_i}} P(y|x, h)P(x)} \right], \tag{14}
 \end{aligned}$$

where $H(x)$ represents information entropy, and h denotes the fading channel coefficients. χ represents the constellation set. \mathcal{O}_{c_i} denotes the constellation subset, where the i -th bit $c_i \in \{0, 1\}$. $m = \log_2 M$.

We give the objective function of the optimized rotation as follows.

Optimization criterion: Given an SNR, select the optimal rotation angle θ^{opt} to maximize the SE

$$\theta^{opt} = \arg \max_{\theta \in [0, 45]} \{I_{BICM}(SNR, \theta)\}. \tag{15}$$

Figures 2–4 show the SE of different rotated angles of θ in 16QAM, 64QAM and 256QAM, respectively, which are obtained from the AMI-optimized criterion by an exhaustive search in Microsoft Visual Studio 2010 software platform. The range of the exhaustive search is from 0 to 45 degrees, and the search interval is set to 0.2 degrees. After passing through the exhaustive search, we can receive the optimal rotated angle θ^{opt} , which can also be obtained through ROC curves by estimating the cutoff points. In Figure 2, when the SNR is 13 dB, the optimal rotated angles θ^{opt} are both 16.8 degrees for the uniform-rotated 16QAM system and the PS-rotated 16QAM system. In Figure 3, when the SNR is 19 dB, the optimal rotated angles θ^{opt} are 8.6 and 12.6 degrees for the uniform-rotated 64QAM system and the PS-rotated 64QAM system, respectively. In Figure 2, when the SNR is 24 dB, the optimal rotated angles θ^{opt} are both 3.6 degrees for the uniform-rotated 256QAM system and the PS-rotated 256QAM system.

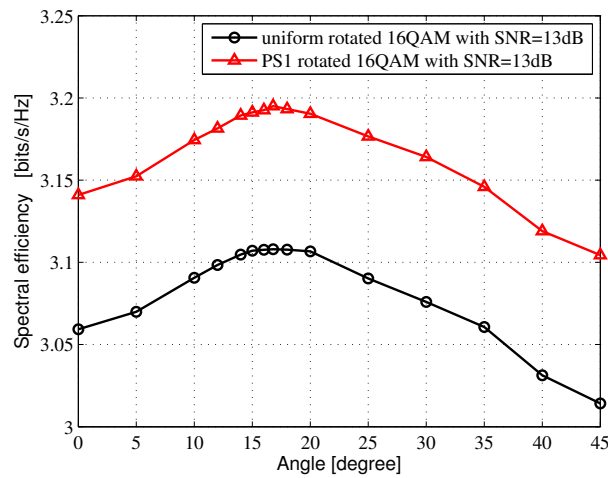


Figure 2. SE vs. θ in 16QAM for Rayleigh fading channel.

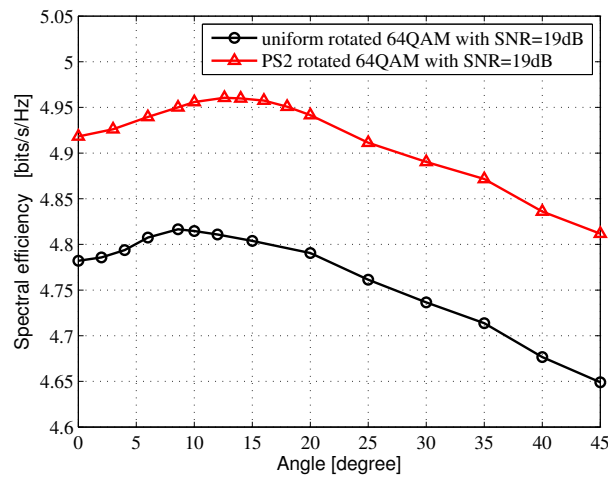


Figure 3. SE vs. θ in 64QAM for Rayleigh fading channel.

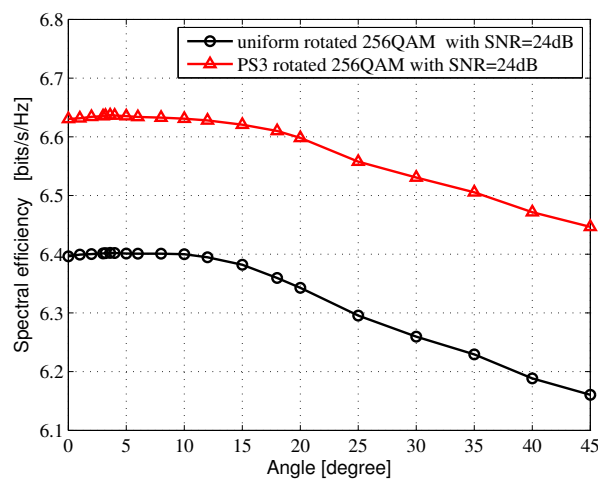


Figure 4. SE vs. θ in 256QAM for Rayleigh fading channel.

Figures 5–7 show the AMI comparison among the uniform QAM with no rotation system, the uniform-rotated QAM system, the PS QAM with no rotation system and the PS-rotated QAM system in Rayleigh fading channel for 16QAM, 64QAM and 256QAM, respectively. The rotation angles are 16.8, 8.6 and 3.6 degrees for uniform 16QAM, uniform

64QAM and uniform 256QAM constellations, respectively, which are also used in the DVB-T2 system for fading channel. In this paper, AMI and SE are equivalent.

For the 16QAM system, we compare the SE at 3.2 bits/s/Hz in Figure 5. Compared with the uniform 16QAM with no rotation system, the uniform-rotated 16QAM with a 16.8-degree rotation system, the PS 16QAM with no rotation system and the PS-rotated 16QAM with a 16.8-degree rotation system can obtain 0.65, 0.12 and 0.75 dB theoretical gains, respectively.

For the 64QAM system, we compare the SE at 4.8 bits/s/Hz in Figure 6. Compared with the uniform 64QAM with no rotation system, the uniform-rotated 64QAM with a 8.6-degree rotation system, the PS 64QAM with no rotation system, the PS-rotated 64QAM with a 8.6-degree rotation system and the PS-rotated 64QAM with the optimal 12.6-degree rotation system can obtain 0.18, 0.29, 0.63 and 0.71 dB theoretical gains, respectively.

For the 256QAM system, we compare the SE at 6.4 bits/s/Hz in Figure 7. Compared with the uniform 256QAM with no rotation system, the uniform-rotated 256QAM with a 3.6-degree rotation system, the PS 256QAM with no rotation system and the PS-rotated 256QAM with a 3.6-degree rotation system can obtain 0.04, 1.0 and 1.04 dB theoretical gains, respectively.

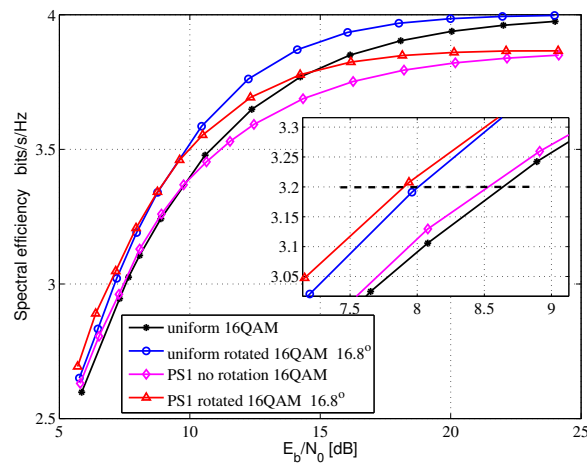


Figure 5. 16QAM AMI for Rayleigh fading channel.

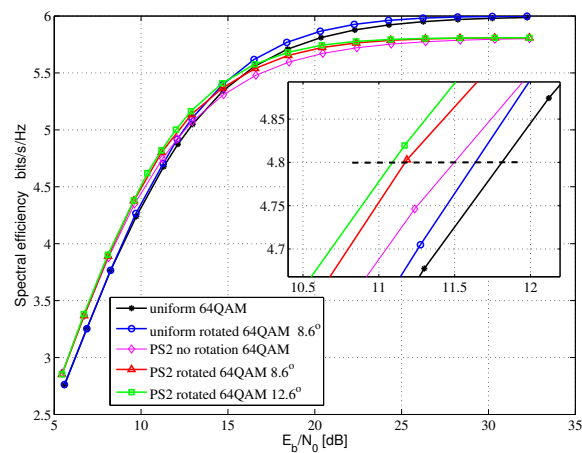


Figure 6. 64QAM AMI for Rayleigh fading channel.

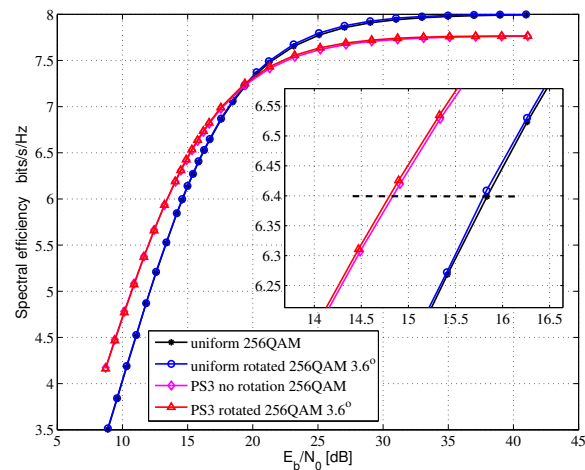


Figure 7. 256QAM AMI for Rayleigh fading channel.

4. Results

We evaluate the performance gain of the proposed NB LDPC-coded PS scheme in Rayleigh fading channel for 16QAM, 64QAM and 256QAM by Monte-Carlo simulations. The simulated software platform is Microsoft Visual Studio 2010. The frame error rate (FER) performance of the end-to-end communication is considered. The NB LDPC codes over GF(16) have an average variable node degree $d_v = 2.4$, while the NB LDPC codes over GF(64) and GF(256) have a regular variable node degree of $d_v = 2$. The LDPC-coded symbol lengths of GF(16), GF(64) and GF(256) are 3000, 2100 and 1500 symbols, respectively. For a fair comparison, the binary LDPC code lengths are 12,000, 12,600 and 12,000 bits in 16QAM, 64QAM and 256QAM, respectively. The binary LDPC codes have a regular variable node degree $d_v = 3$. The LDPC code rate is set to 4/5 for the uniform QAM with no rotation system and the uniform-rotated QAM system, while the LDPC code rate is set to 5/6 for the PS QAM with no rotation system and the PS-rotated QAM system. The total code rate of the system is set to 4/5. The Log-FFT-BP decoding algorithm is considered for NB LDPC codes, while the Log-BP decoding algorithm is considered for binary LDPC codes. The maximum decoding iteration number of NB LDPC codes and binary LDPC codes are both set to 30. The unequal probabilistic amplitudes yield M-B distributions.

Figure 8 shows the FER performance comparisons of 16QAM for Rayleigh fading channel with SE at 3.2 bits/s/Hz. Compared with the uniform GF(2) LDPC-coded 16QAM with no rotation system, the proposed PS GF(2) LDPC-coded 16QAM with a 16.8-degree rotation system can obtain a 0.65 dB performance gain at FER= 10^{-3} . Compared with the uniform GF(16) LDPC-coded 16QAM with no rotation system, the proposed PS GF(16) LDPC-coded 16QAM with a 16.8-degree rotation system can obtain a 0.70 dB performance gain at FER= 10^{-3} . Compared with the uniform GF(2) LDPC-coded 16QAM with no rotation system, the proposed PS GF(16) LDPC-coded 16QAM with a 16.8-degree rotation system can obtain a 1.17 dB performance gain at FER= 10^{-3} .

Figure 9 shows the FER performance comparisons of 64QAM for Rayleigh fading channel with SE at 4.8 bits/s/Hz. Compared with the uniform GF(2) LDPC-coded 64QAM with no rotation system, the proposed PS GF(2) LDPC-coded 64QAM with a 8.6-degree rotation system and the proposed PS GF(2) LDPC-coded 64QAM with the optimal 12.6-degree rotation system can obtain 0.60 and 0.70 dB performance gains at FER= 10^{-3} , respectively. Compared with the uniform GF(64) LDPC-coded 64QAM with no rotation system, the proposed PS GF(64) LDPC-coded 64QAM with the optimal 12.6-degree rotation system can obtain a 0.51 dB performance gain at FER= 10^{-3} . Compared with the uniform GF(2) LDPC-coded 64QAM with no rotation system, the proposed PS GF(64) LDPC-coded 64QAM with the optimal 12.6-degree rotation system can obtain a 1.31 dB performance gain at FER= 10^{-3} .

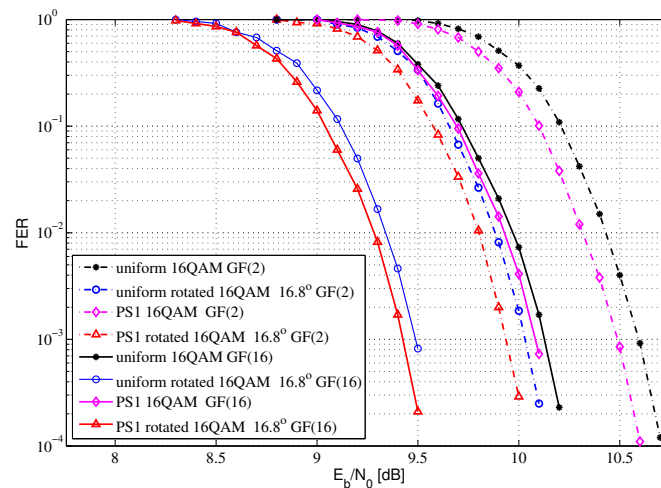


Figure 8. The FER performance of 16QAM for Rayleigh fading channel.

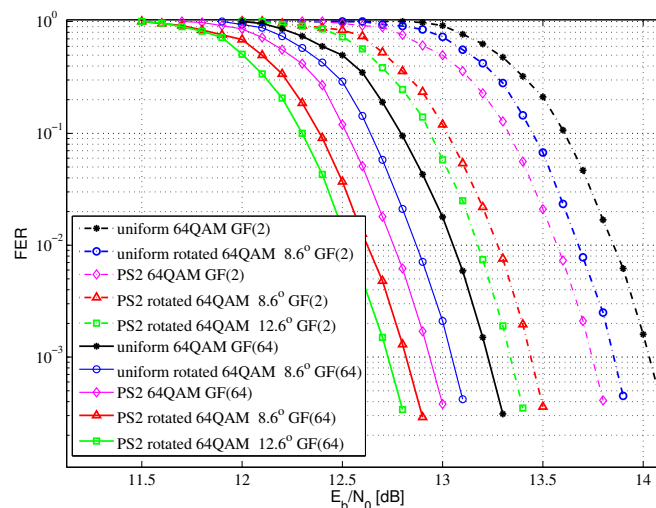


Figure 9. The FER performance of 64QAM for Rayleigh fading channel.

Figure 10 shows the FER performance comparisons of 256QAM for Rayleigh fading channel with SE at 6.4 bits/s/Hz. Compared with the uniform GF(2) LDPC-coded 256QAM with no rotation system, the proposed PS GF(2) LDPC-coded 256QAM with a 3.6-degree rotation system can obtain a 0.77 dB performance gain at FER = 10⁻³. Compared with the uniform GF(256) LDPC-coded 256QAM with no rotation system, the proposed PS GF(256) LDPC-coded 256QAM with a 3.6-degree rotation system can obtain a 0.81 dB performance gain at FER = 10⁻³. Compared with the uniform GF(2) LDPC-coded 256QAM with no rotation system, the proposed PS GF(256) LDPC-coded 256QAM with a 3.6-degree rotation system can obtain a 1.49 dB performance gain at FER = 10⁻³.

In summary, compared with the binary LDPC-coded QAM with no rotation system, the proposed PS nonbinary LDPC-coded QAM with a rotation system can obtain shaping gain, coding gain and diversity gain. In Figures 8–10, there are gaps between the groups of curves, which is due to the selected component.

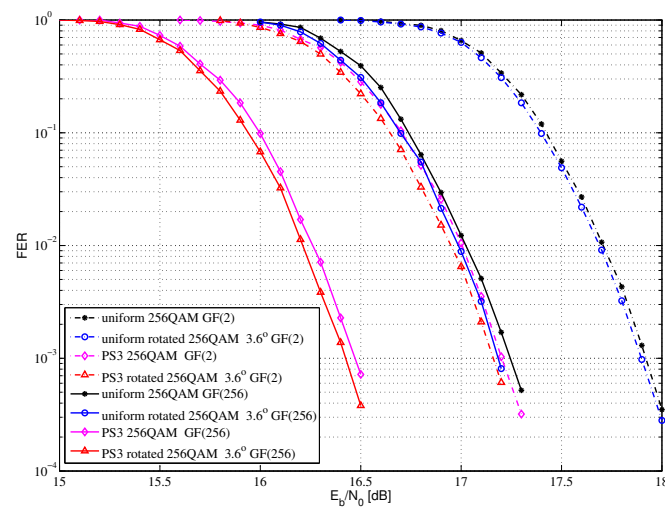


Figure 10. The FER performance of 256QAM for Rayleigh fading channel.

5. Conclusions

In this paper, a NB LDPC-coded PS scheme for Rayleigh fading channel is proposed. The simulation results coincide well with the theoretical AMI analysis, which shows that the NB LDPC-coded PS scheme is suitable for Rayleigh fading channel, and the shaping gain can be obtained. In summary, the proposed NB LDPC-coded PS scheme for Rayleigh fading channel is robust and reliable, which is a potential scheme for the future communication system. In the future, we will consider the Rayleigh flat-fading channel with Doppler shift and consider the question of error protection inequality between the bits transmitted as the sign bits and those represented by the amplitude.

Funding: This work was supported by the Fundamental Research Program of Shanxi Province (202203021212159, 20210302123208).

Institutional Review Board Statement: Not applicable.

Informed Consent Statement: Not applicable.

Data Availability Statement: Not applicable.

Acknowledgments: The author would like to thank the anonymous reviewers for their valuable suggestions and comments.

Conflicts of Interest: The authors declare no conflict of interest.

References

1. Khan, L.U.; Saad, W.; Niyato, D.; Han, Z.; Hong, C.S. Digital-Twin-Enabled 6G: Vision, Architectural Trends, and Future Directions. *IEEE Commun. Mag.* **2022**, *60*, 74–80. [\[CrossRef\]](#)
2. You, L.; Xiong, J.; Ng, D.W.K.; Yuen, C.; Wang, W.; Gao, X. Energy Efficiency and Spectral Efficiency Tradeoff in RIS-Aided Multiuser MIMO Uplink Transmission. *IEEE Trans. Signal Process.* **2021**, *69*, 1407–1421. [\[CrossRef\]](#)
3. Chen, S.; Liang, Y.; Sun, S.; Kang, S.; Cheng, W.; Peng, M. Vision, Requirements, and Technology Trend of 6G: How to Tackle the Challenges of System Coverage, Capacity, User Data-Rate and Movement Speed. *IEEE Wirel. Commun.* **2020**, *27*, 218–228. [\[CrossRef\]](#)
4. Forney, G.; Gallager, R.; Lang, G.; Longstaff, F.; Qureshi, S. Efficient Modulation for Band-Limited Channels. *IEEE J. Sel. Areas Commun.* **1984**, *2*, 632–647. [\[CrossRef\]](#)
5. Bocherer, G.; Steiner, F.; Schulte, P. Bandwidth Efficient and Rate-Matched Low-Density Parity-Check Coded Modulation. *IEEE Trans. Commun.* **2016**, *63*, 4651–4665. [\[CrossRef\]](#)
6. Schulte, P.; Bocherer, G. Constant Composition Distribution Matching. *IEEE Trans. Inf. Theory* **2016**, *62*, 430–434. [\[CrossRef\]](#)
7. Yao, Y.; Xiao, K.; Xia, B.; Gu, Q. Design and Analysis of Rotated-QAM Based Probabilistic Shaping Scheme for Rayleigh Fading Channels. *IEEE Trans. Wirel. Commun.* **2020**, *19*, 3047–3063. [\[CrossRef\]](#)
8. Xiao, K.; Gu, Q.; Xia, B.; Yao, Y. On Rotated-QAM Based Probabilistic Shaping Transmission Scheme for Rayleigh Fading Channels. In Proceedings of the 2019 IEEE 90th Vehicular Technology Conference (VTC2019-Fall), Honolulu, HI, USA, 22–25 September 2019; pp. 1–5.

9. Boutros, J.; Viterbo, E. Signal space diversity: a power- and bandwidth-efficient diversity technique for the Rayleigh fading channel. *IEEE Trans. Inf. Theory* **1998**, *44*, 1453–1467. [[CrossRef](#)]
10. Davey, M.C.; MacKay, D. Low-density parity check codes over GF(q). *IEEE Commun. Lett.* **1998**, *2*, 165–167. [[CrossRef](#)]
11. Steiner, F.; Liva, G.; Bocherer, G. Ultra-Sparse Non-Binary LDPC Codes for Probabilistic Amplitude Shaping. In Proceedings of the GLOBECOM 2017 - 2017 IEEE Global Communications Conference, Singapore, 4–8 December 2017; pp. 1–5.
12. Steiner, F.; Bocherer, G.; Liva, G. Bit-Metric Decoding of Non-Binary LDPC Codes With Probabilistic Amplitude Shaping. *IEEE Commun. Lett.* **2018**, *22*, 2210–2213. [[CrossRef](#)]
13. Kang, W.M. A Novel Nonbinary LDPC-Coded Time Sharing Hybrid Probabilistic Shaping Scheme for 128QAM. In Proceedings of the 2020 IEEE International Conference on Communications Workshops (ICC Workshops), Dublin, Ireland, 7–11 June 2020; pp. 1–6.
14. Hu, X.-Y.; Eleftheriou, E.; Arnold, D.-M. Regular and irregular progressive edge-growth tanner graphs. *IEEE Trans. Inf. Theory* **2005**, *51*, 386–398. [[CrossRef](#)]
15. Wu, Z.; Gao, X.; Jiang, C. Nonbinary LDPC-Coded Spatial Multiplexing for Rate-2 MIMO of DVB-NGH System. *IEEE Trans. Broadcast.* **2018**, *64*, 201–210. [[CrossRef](#)]